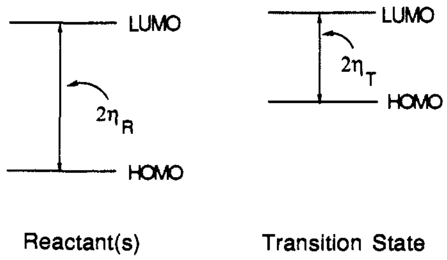

Figure 4. Typical hardness behavior for a chemical reaction: the harder the reactant(s), the more stable it is (they are), and the smaller the reactivity; the harder the transition state, the more stable it is, and the greater the reactivity. Hence the smaller the quantity $\eta_R - \eta_T$ is, the faster the reaction is.

but nontrivial and one that should be investigated further.

Activation hardness as an index of orientation of electrophilic aromatic substitution as here defined considers only the electronic effects. No efforts have been made to include the steric effects that sometimes dictate the amounts of different isomers. But for the molecules we have considered here the electronic effects appear to prevail. Also, we did not consider the effects of the electrophiles. This neglect has been rationalized previously.[33]

A transition state with a large HOMO–LUMO gap, or hardness, is more stable than one with a small gap, and therefore energetically easier to reach. In general, the HOMO–LUMO gap changes as little as possible along the reaction coordinate, as shown in Figure 4. The model theory described in section III and the results given in section IV corroborate these statements.

Activation hardness appears to be an excellent index for predicting the orientation of electrophilic aromatic substitution. *Other things being equal, the softer the reactant is the better, and the harder the transition state is the better.*

Acknowledgment. This work has been aided by research grants from the National Institutes of Health and the National Science Foundation to the University of North Carolina.

---

[33] Reference 2, page 323.

A Theoretical Investigation of the Structures and Properties of Peroxyl Radicals

Susan L. Boyd,[*,†] **Russell J. Boyd,**[‡] **and L. Ross C. Barclay**[§]

Contribution from the Departments of Chemistry, Mount Saint Vincent University, Halifax, Nova Scotia, Canada B3M 2J6, Dalhousie University, Halifax, Nova Scotia, Canada B3H 4J3, and Mount Allison University, Sackville, New Brunswick, Canada E0A 3C0.

Received December 22, 1989

Abstract: As part of a study of the mechanism of the 1,3-migration in allylperoxyl radicals, the equilibrium geometries, dipole moments, charge distributions, spin density distributions, and C–O bond dissociation energies of a variety of peroxyl radicals have been calculated with extended basis sets. It is shown that the effects of electron correlation on the structures of the peroxyl radicals are smaller than in the corresponding peroxides and that electron correlation accounts for about one-half of the C–O bond dissociation energy. The peroxyl radicals are shown to be π-radicals with large dipole moments in the 2.3–2.6 D range. The majority of the negative charge resides on the inner oxygen, while the spin density is higher on the terminal oxygen. The C–O bond dissociation energy decreases with the degree of saturation of the carbon adjacent to the peroxyl group and also when the hydrocarbon radical product is resonance stabilized.

Introduction

Peroxyl radicals are known to form via a variety of chemical processes, including the rapid reaction of oxygen with carbon radicals[1]

$$R^\bullet + O_2 \xrightarrow{k = 10^9\ M^{-1}\ s^{-1}} RO_2^\bullet \qquad (1)$$

Some properties of peroxyls are known. They can be observed directly in solution by ESR, and the unpaired electron in alkyl peroxyls is located in a π-orbital.[2-4] The lifetime of peroxyl radicals may be as long as several seconds at 37 °C,[5] sufficient time for them to diffuse quite freely in solution (and presumably when formed in biological systems). On the other hand, they are sufficiently reactive to abstract hydrogen atoms from C–H bonds and thus are well-known to play a role in the initiation and propagation of free-radical autoxidation of organic substrates.[6-8]

There is renewed interest in oxygen radicals because their attack on lipid biomembranes is related to many important pathological events in biological systems (for typical reviews see references[9-13]). Intrinsic physical properties of peroxyl radicals can affect their behavior in heterogeneous lipid/aqueous systems. For example, a remarkably high polarity has been observed for the benzylperoxyl radical,[14] $\mu = 2.6$ D. It has been suggested that this is due to a significant contribution of dipolar structure **2**.[15] It is argued that

---

[†] Mount Saint Vincent University.

[‡] Dalhousie University.

[§] Mount Allison University.

(1) Maillard, B.; Ingold, K. U.; Scaiano, J. C. *J. Am. Chem. Soc.* **1983**, *105*, 5095.

(2) Howard, J. A. *Can. J. Chem.* **1979**, *57*, 253.

(3) Melamud, E.; Silver, B. *J. Phys. Chem.* **1973**, *77*, 1896.

(4) Adamic, K.; Ingold, K. U.; Morton, J. R. *J. Am. Chem. Soc.* **1970**, *92*, 922.

(5) Pryor, W. A. *Ann. Rev. Physiol.* **1986**, *48*, 657.

(6) Howard, J. A. *Adv. Free Radical Chem.* **1972**, *4*, 49.

(7) Ingold, K. U. *Acc. Chem. Res.* **1969**, *2*, 1.

(8) Mayo, F. R. *Acc. Chem. Res.* **1968**, *1*, 193.

(9) O'Brien, P. J. In *Autoxidation of Unsaturated Lipids*; Academic Press: London, 1987; Chapter 7, pp 233–280.

(10) Halliwell, B.; Gutteridge, J. M. C. *Free Radicals in Biology and Medicine*; Clarendon Press: Oxford, 1985.

(11) Bors, W.; Saran, M.; Tait, D.; Eds.; *Oxygen Radicals in Chemistry and Biology, Proceedings of the 3rd International Conference*; W. de Gruyter & Co.: Berlin, 1984.

(12) McBrien, D. C. H.; Slater, T. F. Eds.; *Protective Agents in Cancer*; Academic Press: New York, 1983.

(13) Pryor, W. A. Ed.; *Free Radicals in Biology*; Academic Press: New York, 1976–1980; Vol. I–V.

(14) Fessenden, R. W.; Hitachi, A.; Nagarajan, V. *J. Phys. Chem.* **1984**, *88*, 107.

0002-7863/90/1512-5724$02.50/0 © 1990 American Chemical Society

1 2

a polarized peroxyl radical (e.g., **2**) could account for some recent observations on the kinetics of autoxidation in microenvironments such as micelles[16] and phospholipid bilayers.[17] Marked reductions in termination rate constants were found in these systems compared to nonaqueous homogeneous solvents. Polar peroxyl radicals are expected to diffuse rapidly from the hydrophobic phases of micelles and bilayers (where they are formed) toward the polar aqueous phase (where hydrogen bonding by water is expected to moderate their recombination rate). We speculate that this behavior of polar peroxyl radicals may explain, in part, the ability of some water-soluble chain-breaking antioxidants to inhibit autoxidations initiated in the hydrophobic phase of membranes.[17-20] The mode of such antioxidant action in biphasic systems could involve inhibition of autoxidation in the membrane phase by trapping peroxyl radicals at or near the aqueous/membrane surface.

The detailed mechanism of peroxidation of unsaturated lipids, a subject of continuing great interest, implicates carbon-to-oxygen β-bond scission[21] (e.g., the reverse of reaction 1), which has been observed for the allylperoxyl system[22] and a few other peroxyls.[23] A knowledge of the carbon-to-oxygen bond energy for peroxyls of varying R-groups would be important to peroxyl radical chemistry in several respects. It would provide useful data for the energetics of rearrangement of allyl peroxyl radicals (2), a

(2)

subject of current interest to a number of investigators.[23-26] Such data should also clarify to some extent the complexities of peroxidation of polyunsaturated lipids, known to involve competition of peroxyl radicals for hydrogen abstraction, β-scission, and cyclization (3), the latter being important to the formation of prostaglandin endoperoxide in biological systems.[27]

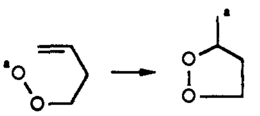

(3)

In this paper we present results of ab initio calculations on the structures and properties of peroxyl radicals. The structures are fully optimized at the 6-31G* level; properties include dipole moments, charge distributions (Mulliken population analyses), and spin densities. The C–O bond energies of many of the peroxy radicals are presented.

Computational Methods

Calculations were performed at the unrestricted Hartree–Fock (denoted by HF throughout this paper), MP2 and MP3 (second- and third-order Møller–Plesset) levels by using the GAUSSIAN 80[28] and GAUSSIAN 86[29] computer programs. Standard 6-31G* basis sets[30] were used for all geometry optimizations, and most of the results are discussed with reference to this level of calculation. In addition, some of the smaller structures were optimized at the MP2/6-31G* level.[31] Bond dissociation energies were determined at the MP2/6-311G**//HF/6-31G* level for all one- or two-carbon and some three-carbon species and at the MP2/6-31G**//HF/6-31G* levels for all species.[31]

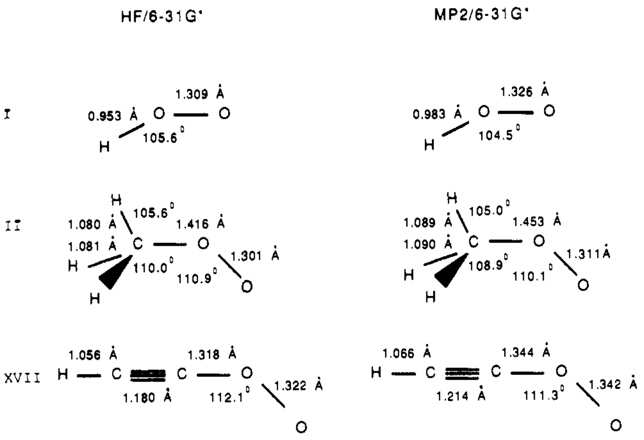

Figure 1. The effect of electron correlation on equilibrium geometries. The structures of all radicals were fully optimized at both the 6-31G* level and the MP2/6-31G* level.

We have used the standard notation, A//B, to indicate that the property of interest has been calculated at theoretical level A by using the equilibrium geometry obtained at level B. Strictly speaking, all calculations denoted by HF would be more appropriately denoted by SCF (self-consistent field) because the sizes of the species necessitate the use of incomplete basis sets; we have, however, followed the standard practice of referring to self-consistent field calculations with finite basis sets as either HF or SCF calculations.

Results and Discussion

In order to ascertain the effect of electron correlation on the structures of peroxyl radicals, equilibrium geometries for three peroxy radicals were optimized at both the HF/6-31G* and the MP2/6-31G* levels; the results are presented in Figure 1. As has been noted for other systems,[32] the effect of electron correlation in all the peroxy radicals studied is to increase bond lengths and reduce bond angles; however, the change is generally less than that in the corresponding peroxides. For example, in the HOO• radical, the O–O bond length increases by only 1.3% in going from the HF/6-31G* optimization to the MP2/6-31G* optimization (1.309 Å → 1.326 Å), whereas, in hydrogen peroxide the O–O bond length goes up by 5.3% (1.393 Å → 1.467 Å).[33] The HOO bond angle decreases by about 1.0% in the peroxyl radical (105.6° → 104.5°), while in H_2O_2 the decrease is 3.4% (102.2° → 98.7°). However in both $HO_2^\bullet$ and H_2O_2, the O–H bond length decrease is about 3% (0.953 Å → 0.983 Å in the radical, 0.949 Å → 0.976 Å in the molecular species). Similar trends are evident for both the methylperoxyl radical and the ethynylperoxyl radical (Figure 1).

Thus, while it is known that the effect of electron correlation on equilibrium geometries tends to be greatest for bonds involving small electronegative atoms,[34] the present calculations indicate that the correlation effects are smaller in the peroxyl radicals than

---

[15] Barclay, L. R. C.; Ingold, K. U. *J. Am. Chem. Soc.* **1981**, *103*, 6478.

[16] Barclay, L. R. C.; Baskin, K. A.; Locke, S. J.; Schaefer, T. D. *Can. J. Chem.* **1987**, *65*, 2529.

[17] Barclay, L. R. C.; Baskin, K. A.; Locke, S. J.; Vinquist, M. R. *Can. J. Chem.* **1989**, *67*, August.

[18] Niki, E. *Chem. Phys. Lipids* **1987**, *44*, 227.

[19] Burton, G. W.; Ingold, K. U. *Acc. Chem. Res.* **1986**, *19*, 194.

[20] Barclay, L. R. C.; Locke, S. J.; MacNeil, J. M.; VanKessel, J.; Burton, G. W.; Ingold, K. U. *J. Am. Chem. Soc.* **1984**, *106*, 2479.

[21] Porter, N. A. *Acc. Chem. Res.* **1986**, *19*, 262.

[22] Morgan, C. A.; Pilling, M. J.; Tulloch, J. M. *J. Chem. Soc., Faraday Trans. 2* **1982**, *78*, 1323.

[23] Porter, N. A.; Wujek, J. S. *J. Org. Chem.* **1987**, *52*, 5085.

[24] Beckwith, A. L. J.; Davies, A. G.; Davison, G. E.; Maccoll, A.; Mruzek, M. H. *J. Chem. Soc., Perkin Trans. II* **1989**, 815.

[25] Porter, N. A.; Zuraw, P. *J. Chem. Soc., Chem. Commun.* **1985**, 1472.

[26] Brill, W. F. *J. Chem. Soc., Perkin Trans. II* **1984**, 621.

[27] Porter, N. A. In *Free Radicals in Biology*; Pryor, W. A., Ed.; Academic Press: New York, 1980; Vol. IV, pp 261–294.

[28] Binkley, J. S.; Whiteside, R. A.; Krishnan, R.; Seeger, R.; DeFrees, D. J.; Schlegel, H. B.; Topiol, S.; Kahn, L. R.; Pople, J. A. GAUSSIAN 80; Carnegie-Mellon Quantum Chemistry Publishing Unit: Pittsburgh, PA.

[29] Frisch, M. J.; Binkley, J. S.; Schlegel, H. B.; Raghavachari, K.; Melius, C. F.; Martin, R. L.; Stewart, J. J. P.; Bobrowicx, F. W.; Rohlfing, C. M.; Kahn, L. R.; DeFrees, D. J.; Seeger, R.; Whiteside, R. A.; Fox, D. J.; Fleuder, E. M.; Pople, J. A. GAUSSIAN 86; Carnegie-Mellon Quantum Chemistry Publishing Unit; Pittsburgh, PA, 1984.

[30] Hehre, W. J.; Radom, L.; Schleyer, P. v. R.; Pople, J. A. *Ab Initio Molecular Orbital Theory*; Wiley: New York, 1986; p 82.

[31] Reference 30, p 90.

[32] Reference 30, pp 194–197.

[33] reference 30, p 159.

[34] DeFrees, D. J.; Levi, B. A.; Pollack, S. K.; Hehre, W. J.; Binkley, J. S.; Pople, J. A. *J. Am. Chem. Soc.* **1979**, *101*, 4085.

Table I. Calculated Structural Parameters, Charge Distributions, Spin Densities, Dipole Moments, Total Energies, and Relative Energies of Conformers at the 6-31G* Level

	molecule	point group	bond length (Å)	bond angles (deg)	state	charge distribution	spin density	dipole moment (D)	total energy (au)	relative energy (kJ/mol)
I	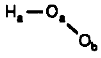	C_s	H_aO_a 0.953 O_aO_b 1.309	$H_aO_aO_b$ 105.6	$^2A''$	H_a +0.468 O_a −0.392 O_b −0.076	H_a −0.011 O_a +0.090 O_b +0.921	2.10	−150.17053	
II	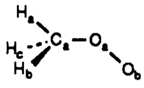	C_s	H_aC_a 1.080 H_bC_a 1.081 C_aO_a 1.416 O_aO_b 1.301	$H_aC_aO_a$ 105.6 $H_bC_aO_a$ 110.0 $H_aC_aH_b$ 110.4 $H_bC_aH_c$ 110.3 $C_aO_aO_b$ 110.9	$^2A''$	H_a +0.189 H_b +0.182 C_a −0.176 O_a −0.296 O_b −0.079	H_a −0.002 H_b +0.009 C_a −0.023 O_a +0.104 O_b +0.904	2.45	−189.20232	0
III	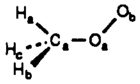	C_s	H_aC_a 1.079 H_bC_a 1.081 C_aO_a 1.421 O_aO_b 1.301	$H_aC_aO_a$ 109.3 $H_bC_aO_a$ 108.2 $H_aC_aH_b$ 109.0 $H_bC_aH_c$ 107.4 $C_aO_aO_b$ 112.5	$^2A''$	H_a +0.194 H_b +0.184 C_a −0.186 O_a −0.292 O_b −0.082	H_a −0.002 H_b +0.003 C_a −0.019 O_a +0.127 O_b +0.889	2.49	−189.20019	5.6
IV	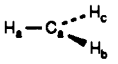	C_{3v}	H_aC_a 1.073	$H_aC_aH_b$ 120.0	$^2A_1$	H_a +0.175 C_a −0.525	H_a −0.099 C_a +1.298	0	−39.55899	
V	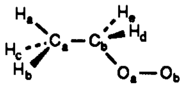	C_s	H_aC_a 1.084 H_bC_a 1.084 C_aC_b 1.514 C_bH_d 1.083 C_bO_a 1.421 O_aO_b 1.301	$H_aC_aC_b$ 109.8 $H_bC_aC_b$ 110.8 $H_aC_aH_b$ 108.7 $H_bC_aH_c$ 108.1 $C_aC_bH_d$ 111.6 $C_aC_bO_a$ 107.8 $H_dC_bH_a$ 107.3 $H_dC_bO_a$ 109.3 $C_bO_aO_b$ 111.3	$^2A''$	H_a +0.175 H_b +0.186 H_d +0.175 C_a −0.516 C_b +0.005 O_a −0.312 O_b −0.074	H_a −0.001 H_b 0 H_d +0.008 C_a −0.001 C_b −0.022 O_a +0.104 O_b +0.904	2.53	−228.24256	0
VI	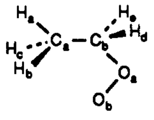	C_s	H_aC_a 1.085 H_bC_a 1.083 C_aC_b 1.516 C_bH_d 1.083 C_bO_a 1.435 O_aO_b 1.294	$H_aC_aC_b$ 108.4 $H_bC_aC_b$ 111.5 $H_aC_aH_b$ 109.0 $H_bC_aH_c$ 107.4 $C_aC_bH_d$ 111.0 $C_aC_bO_a$ 115.2 $H_dC_bH_c$ 107.9 $H_dC_bO_a$ 105.7 $C_bO_aO_b$ 114.7	$^2A''$	H_a +0.171 H_b +0.188 H_d +0.180 C_a −0.511 C_b −0.002 O_a −0.308 O_b −0.086	H_a −0.001 H_b 0 H_d +0.005 C_a −0.001 C_b −0.024 O_a +0.139 O_b +0.878	2.57	−228.23719	14
VII	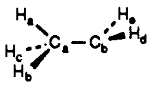	C_s	H_aC_a 1.091 H_bC_a 1.086 C_aC_b 1.498 C_bH_d 1.075	$H_aC_aC_b$ 111.7 $H_bC_aC_b$ 111.3 $H_aC_aH_b$ 107.1 $H_bC_aH_c$ 108.0 $C_aC_bH_d$ 120.4 $H_dC_bH_c$ 117.3	$^2A'$	H_a +0.166 H_b +0.168 H_d +0.167 C_a −0.496 Cb −0.340	H_a +0.060 H_b +0.016 H_d −0.096 C_a −0.160 C_b +1.259	0.22	−78.59714	
VIII	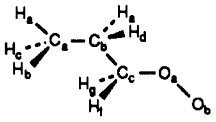	C_s	H_aC_a 1.084 H_bC_a 1.086 C_aC_b 1.531 C_bH_d 1.085 C_bC_c 1.518 C_cH_f 1.084 C_cO_a 1.420 O_aO_b 1.301	$H_aC_aC_b$ 110.8 $H_aC_aH_b$ 107.8 $H_bC_aH_c$ 107.6 $H_bC_aC_b$ 111.3 $H_dC_bH_e$ 109.6 $C_aC_bC_c$ 110.6 $H_dC_bC_c$ 108.9 $C_bC_cH_f$ 111.4 $C_aC_bH_d$ 109.3 $H_fC_cH_g$ 107.2 $H_fC_cO_a$ 109.4 $C_bC_cO_a$ 108.2 $C_cO_aO_b$ 111.3	$^2A''$	H_a +0.178 H_b +0.166 H_d +0.183 H_f +0.172 C_a −0.498 C_b −0.343 C_c +0.021 O_a −0.322 O_b −0.075	H_a 0 H_b 0 H_d 0 H_f +0.008 C_a −0.001 C_b −0.001 C_c −0.022 O_a +0.105 O_b +0.904	2.62	−267.27692	
IX	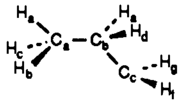	C_s	H_aC_a 1.085 H_bC_a 1.086 C_aC_b 1.537 C_bH_d 1.087 C_bC_c 1.503 C_cH_f 1.076	$H_aC_aC_b$ 111.7 $H_aC_aH_b$ 108.6 $H_bC_aH_c$ 106.4 $H_bC_aC_b$ 110.7 $H_dC_bH_c$ 107.8 $C_aC_bC_c$ 112.6 $H_dC_bC_c$ 108.9 $C_bC_cH_f$ 120.3 $H_fC_cH_g$ 117.1	$^2A'$	H_a +0.160 H_b +0.158 H_d +0.164 H_f +0.166 C_a −0.473 C_b −0.321 C_c −0.341	H_a +0.009 H_b −0.003 H_d +0.016 H_f −0.096 C_a +0.051 C_b −0.159 C_c +1.266	0.21	−117.63127	
X	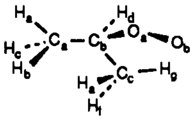	C_s	H_aC_a 1.085 H_bC_a 1.084 C_aC_b 1.520 C_bH_d 1.083 C_bO_a 1.436 O_aO_b 1.301	$H_aC_aC_b$ 109.9 $H_aC_aH_b$ 108.3 $H_aC_aH_c$ 108.4 $H_bC_aH_c$ 108.4 $C_aC_bH_d$ 109.6 $C_aC_bO_a$ 110.6 $H_dC_bO_a$ 101.8 $C_bO_aO_b$ 112.2 $C_aC_bC_c$ 113.9	$^2A''$	H_a +0.167 H_b +0.186 H_c +0.183 H_d +0.187 C_a −0.502 C_b +0.148 O_a −0.317 O_b −0.086	H_a −0.003 H_b −0.001 H_c 0 H_d −0.002 C_a +0.009 C_b −0.019 O_a +0.113 O_b +0.898	2.53	−267.28131	

Table I (Continued)

	molecule	point group	bond length (Å)	bond angles (deg)	state	charge distribution	spin density	dipole moment (D)	total energy (au)	relative energy (kJ/mol)
XI	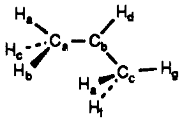	C_{2v}	H_aC_a 1.084 H_bC_a 1.090 C_aC_b 1.499 C_bH_d 1.075	$H_aC_aC_b$ 111.7 $H_aC_aH_b$ 107.7 $H_bC_aH_c$ 106.6 $C_aC_bH_d$ 119.7 $C_aC_bC_c$ 120.5	$^2B_1$	H_a +0.167 H_b +0.162 H_d +0.176 C_a −0.497 C_b −0.165	H_a +0.007 H_b +0.048 H_d −0.103 C_a −0.174 C_b +1.244	0.02	−117.63561	
XII	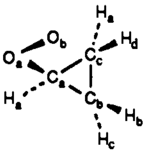	C_s	H_aC_a 1.072 C_aC_b 1.484 C_bH_b 1.074 C_bH_c 1.076 C_bC_c 1.509 C_aO_a 1.411 O_aO_b 1.296	$H_aC_aC_b$ 120.2 $H_aC_aO_a$ 106.8 $C_aC_bC_c$ 58.9 $C_aC_bH_b$ 117.0 $H_bC_bH_c$ 114.9 $C_aO_aO_b$ 113.5 $C_bC_aC_c$ 61.1 $C_aC_bH_c$ 118.3 $C_aC_bC_c$ 113.9	$^2A''$	H_a +0.209 H_b +0.214 H_c +0.193 C_a +0.154 C_b −0.394 O_a −0.310 O_b −0.081	H_a −0.001 H_b −0.002 H_c −0.002 C_a −0.030 C_b +0.016 O_a +0.122 O_b +0.886	2.39	−266.06865	
XIII	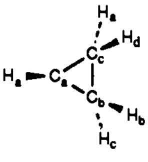	C_s	H_aC_a 1.072 C_aC_b 1.470 C_bH_b 1.078 C_bH_c 1.078 C_bC_c 1.517	$H_aC_aC_b$ 130.3 $C_aC_bC_c$ 56.6 $C_aC_bH_b$ 119.1 $C_aC_bH_c$ 118.3 $H_bC_bH_c$ 113.9 $C_bC_aC_c$ 62.1	$^2A'$	H_a +0.181 H_b +0.181 H_c +0.187 C_a −0.160 C_b −0.379	H_a −0.052 H_b +0.023 H_c +0.031 C_a +1.153 C_b −0.105	0.54	−116.41553	
XIV	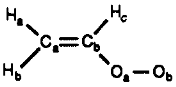	C_s	H_aC_a 1.072 H_bC_a 1.074 C_aC_b 1.316 C_bH_c 1.071 C_bO_a 1.375 O_aO_b 1.298	$H_aC_aC_b$ 119.8 $H_aC_aH_b$ 118.5 $H_bC_aC_b$ 121.7 $C_aC_bH_c$ 126.3 $C_aC_bO_a$ 120.2 $H_cC_bO_a$ 113.5 $C_bO_aO_b$ 112.6	$^2A''$	H_a +0.200 H_b +0.209 H_c +0.223 C_a −0.454 C_b +0.185 O_a −0.294 O_b −0.069	H_a −0.027 H_b −0.028 H_c +0.021 C_a +0.371 C_b −0.343 O_a +0.119 O_b +0.886	2.06	−227.04727	0
XV	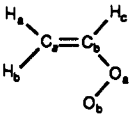	C_s	H_aC_a 1.073 H_bC_a 1.071 C_aC_b 1.317 C_bH_c 1.071 C_bO_a 1.376 O_aO_b 1.300	$H_aC_aC_b$ 118.8 $H_aC_aH_b$ 118.5 $H_bC_aC_b$ 122.7 $C_aC_bH_c$ 124.9 $C_aC_bO_a$ 126.8 $H_cC_bO_a$ 108.3 $C_bO_aO_b$ 114.6	$^2A''$	H_a +0.197 H_b +0.218 H_c +0.219 C_a −0.443 C_b +0.168 O_a −0.307 O_b −0.051	H_a −0.027 H_b −0.027 H_c −0.022 C_a +0.375 C_b −0.343 O_a +0.096 O_b +0.905	2.01	−227.04606	3
XVI	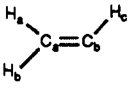	C_s	H_aC_a 1.080 H_bC_a 1.077 C_aC_b 1.328 C_bH_c 1.071	$H_aC_aC_b$ 121.9 $H_aC_aH_b$ 116.6 $H_bC_aC_b$ 121.9 $C_aC_bH_c$ 134.6	$^2A'$	H_a +0.185 H_b +0.189 H_c +0.192 C_a −0.395 C_b −0.171	H_a +0.119 H_b +0.082 H_c −0.062 C_a −0.861 C_b +1.722	0.58	−77.39028	
XVII	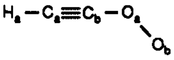 $H_a{-}C_a{\equiv}C_b{-}O_a{-}O_b$	C_s	H_aC_a 1.056 C_aC_b 1.180 C_bO_a 1.318 O_aO_b 1.322	$H_aC_aC_b$ 180.0 $C_aC_bO_a$ 180.0 $C_bO_aO_b$ 112.1	$^2A''$	H_a +0.293 C_a −0.145 C_b +0.195 O_a −0.330 O_b −0.013	H_a −0.003 C_a +0.050 C_b −0.054 O_a +0.060 O_b −0.947	1.41	−225.80859	
XVIII	$H_a{-}C_a{\equiv}C_b$	$C_{\infty v}$	H_aC_a 1.058 C_aC_b 1.215	$H_aC_aC_b$ 180.0	$^2\Sigma$	H_a +0.271 C_a −0.176 C_b −0.094	H_a +0.104 C_a −1.249 C_b +2.144	0.72	−76.15008	
XIX	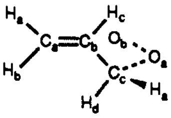	C_1	H_aC_a 1.075 H_bC_a 1.077 C_aC_b 1.318 C_bH_c 1.078 C_bC_c 1.498 C_cH_d 1.083 C_cH_e 1.081 C_cO_a 1.426 O_aO_b 1.302	$H_aC_aC_b$ 121.6 $H_bC_aC_b$ 121.9 $H_aC_aH_b$ 116.5 $C_aC_bH_c$ 120.5 $C_aC_bC_c$ 124.1 $H_cC_bC_c$ 115.4 $C_bC_cH_d$ 113.2 $C_bC_cH_e$ 109.9 $H_dC_cH_e$ 109.3 $C_bC_cO_a$ 111.6 $H_dC_cO_a$ 107.4 $H_eC_cO_a$ 105.0 $C_cO_aO_b$ 111.1 $C_aC_bC_cO_a$ 124.5 $C_bC_cO_aO_b$ 74.5	^2A	H_a +0.189 H_b +0.184 H_c +0.202 H_d +0.191 H_e +0.195 C_a −0.378 C_b −0.156 C_c −0.042 O_a −0.311 O_b −0.074	H_a +0.010 H_b +0.009 H_c −0.009 H_d +0.007 H_e +0.007 C_a −0.133 C_b +0.135 C_c −0.032 O_a +0.106 O_b +0.907	2.51	−266.08236	0
XX	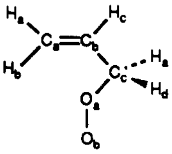	C_s	H_aC_a 1.074 H_bC_a 1.074 C_aC_b 1.317 C_bH_c 1.078 C_bC_c 1.499 C_cH_d 1.084 C_cO_a 1.419 O_aO_b 1.300	$H_aC_aC_b$ 120.7 $H_bC_aC_b$ 122.3 $H_aC_aH_b$ 117.0 $C_aC_bH_c$ 120.0 $C_aC_bC_c$ 126.2 $H_cC_bC_c$ 113.8 $C_bC_cH_d$ 110.9 $H_dC_cH_c$ 108.2 $C_bC_cO_a$ 109.6 $H_dC_cO_a$ 108.6 $C_cO_aO_b$ 110.9	$^2A''$	H_a +0.184 H_b +0.210 H_c +0.192 H_d +0.186 C_a −0.376 C_b −0.200 C_c +0.010 O_a −0.324 O_b −0.068	H_a +0.002 H_b +0.001 H_c −0.002 H_d +0.009 C_a −0.021 C_b +0.020 C_c −0.025 O_a +0.105 O_b +0.903	2.34	−266.08121	3

Table I (Continued)

	molecule	point group	bond length (Å)	bond angles (deg)	state	charge distribution	spin density	dipole moment (D)	total energy (au)	relative energy (kJ/mol)
XXI	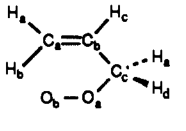	C_s	H_aC_a 1.076 H_bC_a 1.069 C_aC_b 1.319 C_bH_c 1.080 C_bC_c 1.504 C_cH_d 1.084 C_cO_a 1.429 O_aO_b 1.292	$H_aC_aC_b$ 118.9 $H_bC_aC_b$ 124.2 $H_aC_aH_b$ 116.9 $C_aC_bH_c$ 117.3 $C_aC_bC_c$ 133.9 $H_cC_bC_c$ 108.8 $C_bC_cH_d$ 108.5 $H_dC_cH_e$ 107.1 $C_bC_cO_a$ 122.0 $H_dC_cO_a$ 104.9 $C_cO_aO_b$ 116.7	$^2A''$	H_a +0.178 H_b +0.217 H_c +0.183 H_d +0.192 C_a −0.375 C_b −0.191 C_c −0.005 O_a −0.312 O_b −0.079	H_a −0.005 H_b −0.005 H_c +0.004 H_d +0.004 C_a +0.058 C_b −0.055 C_c −0.019 O_a +0.138 O_b +0.879	2.42	−266.06844	36
XXII	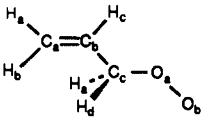	C_s	H_aC_a 1.075 H_bC_a 1.077 C_aC_b 1.317 C_bH_c 1.076 C_bC_c 1.505 C_cH_d 1.082 C_cO_a 1.424 O_aO_b 1.300	$H_aC_aC_b$ 121.3 $H_bC_aC_b$ 122.3 $H_aC_aH_b$ 116.4 $C_aC_bH_c$ 120.5 $C_aC_bC_c$ 124.2 $H_cC_bC_c$ 115.3 $C_bC_cH_d$ 112.0 $H_dC_cH_c$ 108.9 $C_bC_cO_a$ 106.9 $H_dC_cO_a$ 108.4 $C_cO_aO_b$ 111.1	$^2A''$	H_a +0.191 H_b +0.178 H_c +0.218 H_d +0.194 C_a −0.393 C_b −0.184 C_c +0.002 O_a −0.332 O_b −0.068	H_a +0.003 H_b +0.003 H_c −0.003 H_d +0.010 C_a −0.042 C_b +0.039 C_c −0.027 O_a +0.104 O_b +0.903	2.39	−266.07927	8
XXIII	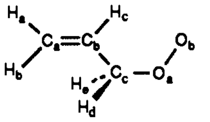	C_s	H_aC_a 1.075 H_bC_a 1.078 C_aC_b 1.320 C_bH_c 1.071 C_bC_c 1.507 C_cH_d 1.082 C_cO_a 1.437 O_aO_b 1.293	$H_aC_aC_b$ 121.1 $H_bC_aC_b$ 122.6 $H_aC_aH_b$ 116.3 $C_aC_bH_c$ 120.3 $C_aC_bC_c$ 122.2 $H_cC_bC_c$ 117.5 $C_bC_cH_d$ 111.0 $H_dC_cH_c$ 108.2 $C_bC_cO_a$ 116.3 $H_dC_cO_a$ 105.0 $C_cO_aO_b$ 116.1	$^2A''$	H_a +0.190 H_b +0.176 H_c +0.236 H_d +0.198 C_a −0.391 C_b −0.199 C_c −0.011 O_a −0.315 O_b −0.083	H_a −0.016 H_b −0.016 H_c +0.014 H_d −0.002 C_a +0.226 C_b −0.222 C_c +0.001 O_a +0.140 O_b +0.877	2.43	−266.07216	27
XXIV	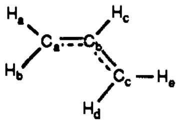	C_{2v}	H_aC_a 1.074 H_bC_a 1.076 C_aC_b 1.391 C_bH_c 1.078	$H_aC_aC_b$ 121.4 $H_bC_aC_b$ 121.2 $H_aC_aH_b$ 117.4 $C_aC_bH_c$ 117.7 $C_aC_bC_c$ 124.6	$^2A_2$	H_a +0.179 H_b +0.176 H_c +0.184 C_a −0.379 C_b −0.135	H_a −0.079 H_b −0.076 H_c +0.050 C_a +1.027 C_b −0.795	0.04	−116.46810	
XXV	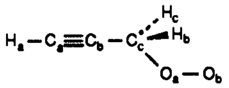	C_s	H_aC_a 1.057 C_aC_b 1.185 C_bC_c 1.464 C_cH_b 1.081 C_cO_a 1.424 O_aO_b 1.300	$H_aC_aC_b$ 180.0 $C_aC_bC_c$ 180.0 $C_bC_cH_b$ 110.9 $H_bC_cH_c$ 109.2 $C_bC_cO_a$ 108.1 $C_cO_aO_b$ 110.1 $H_bC_cO_a$ 108.8	$^2A''$	H_a +0.300 H_b +0.214 C_a −0.477 C_b +0.114 C_c +0.003 O_a −0.302 O_b −0.065	H_a +0.001 H_b +0.009 C_a −0.026 C_b +0.023 C_c −0.025 O_a +0.103 O_b +0.906	2.37	−264.86850	0
XXVI	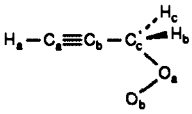	C_s	H_aC_a 1.057 C_aC_b 1.185 C_bC_c 1.464 C_cH_b 1.082 C_cO_a 1.432 O_aO_b 1.295	$H_aC_aC_b$ 180.0 $C_aC_bC_c$ 180.0 $C_bC_cH_b$ 110.3 $H_bC_cH_c$ 108.5 $C_bC_cO_a$ 115.3 $C_cO_aO_b$ 115.3 $H_bC_cO_a$ 106.1	$^2A''$	H_a +0.297 H_b +0.217 C_a −0.465 C_b +0.109 C_c −0.005 O_a −0.313 O_b −0.056	H_a 0 H_b +0.004 C_a +0.002 C_b −0.003 C_c −0.022 O_a +0.122 O_b +0.893	2.38	−264.86257	16
XXVII	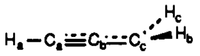	C_{2v}	H_aC_a 1.057 C_aC_b 1.218 C_bC_c 1.382 C_cH_b 1.074	$H_aC_aC_b$ 180.0 $C_aC_bC_c$ 180.0 $C_bC_cH_b$ 120.7 $H_bC_cH_c$ 118.6	$^2B_1$	H_a +0.290 H_b −0.204 C_a −0.408 C_b +0.127 C_c −0.417	H_a −0.072 H_b −0.097 C_a +1.178 C_b −1.072 C_c +1.159	0.10	−115.25060	

in the corresponding peroxides. This is fortunate because it is impractical to carry out MP2 optimizations for the larger systems. Accordingly, the properties discussed below have been calculated at the HF/6-31G* optimized geometries.

The geometries of both the peroxyl radicals and the corresponding hydrocarbon radicals (eq 1), determined at the 6-31G* level, are tabulated in Table I. In addition, Table I shows the charge distributions (from Mulliken population analyses), the electronic states, the spin densities, and the dipole moments of the peroxyl and the hydrocarbon radicals.

As is apparent from Table I, the C–O bond length is essentially the same for all species in which the oxygen is bonded to a saturated carbon (1.41–1.43 Å). It decreases for the ethenylperoxyl radical (XIV) to 1.38 Å and further yet for the ethynylperoxyl radical (XVII) to 1.32 Å. This trend is consistent with the qualitative trend of decreasing bond length with increasing s-character of the bonding molecular orbital. The O–O bond length is essentially constant (1.30 Å) throughout the structures investigated, with only one species slightly deviating from this (1.32 Å in the ethynylperoxyl radical, XVII). The COO bond angle varies from 110.1° to 116.7°, with the more open angles corresponding to more sterically hindered structures, e.g., XXI, XXIII, and XXVI.

As has been noted experimentally,[2-4] the electronic state of all peroxyl radicals of C_s symmetry is $^2A''$, i.e., the radicals are π-radicals. This is not surprising since one can envision that the

Table II. Bond Dissociation Energies for Loss of O_2

$$R\text{–}O\text{–}O^{\bullet} \rightarrow R^{\bullet} + O_2$$

		bond dissociation energies (kJ/mol)							
	peroxyl radical	6-31G* SCF	6-31G**//HF/6-31G* SCF	6-31G**//HF/6-31G* MP2	6-31G**//HF/6-31G* MP3	6-311G**//HF/6-31G* SCF	6-311G**//HF/6-31G* MP2	6-311G**//HF/6-31G* MP3	exp[a]
I	$HOO^{\bullet}$	143	159	179	205	155	173	201	223 (197)
II	$CH_3O_2^{\bullet}$	67	65	124	130	60	110	119	135 (109)
V	$C_2H_5O_2^{\bullet}$	72	71	134	138	67	121		139 (117)
									146 (124)[b]
VIII	1° $C_3H_7O_2^{\bullet}$	73	72	136		68			
X	2° $C_3H_7O_2^{\bullet}$	73	72	146					143 (121)
XIV	$C_2H_3O_2^{\bullet}$	103	102	200	199	97	186	186	
XVII	$C_2HO_2^{\bullet}$	106	107	235	227	105	226	221	
XVIII	$C_3H_5O_2^{\bullet}$	−10	−11	89					83 (63)
XXV	$C_3H_3O_2^{\bullet}$	0	−1	102		−4	89		

[a] Experimental D_0 values (from ref 37 except where otherwise noted) have been converted to D_e values by using the scaled 6-31G* vibrational frequencies to estimate the zero-point correction.[39] The uncorrected D_0 values are given in parentheses. [b] Based on D_0 from ref 38.

peroxyl radical results from the bonding of a σ-alkyl radical and an O_2-diradical (which has its two unpaired electrons in π-orbitals), leaving the unpaired electron in the peroxyl radical in a π-molecular orbital.

The peroxyl radicals all exhibit relatively high dipole moments, typically greater than 2 D and generally in the range 2.3–2.6 D. This is consistent with the experimentally observed dipole moment of 2.6 D for the benzylperoxyl radical;[14] thus peroxyl radicals are considerably more polar than water (μ = 1.85 D). The *least* polar is the ethynylperoxyl radical, XVII (μ = 1.41 D); the corresponding ethynyl radical XVIII is the most polar of the hydrocarbon radicals (μ = 0.72 D). The s-*trans*- and s-*cis*-ethenylperoxyl radicals, XIV and XV, have the second lowest dipole moments of the peroxyl radicals studied (μ = 2.06 and 2.01 D, respectively); similarly, the ethenyl radical XVI has the second highest dipole moment of the alkyl radicals studied (μ = 0.58 D). The relative magnitudes and directions of the dipole moments for the peroxyl species containing two carbons are shown schematically in Figure 2.

In all cases, the charge distribution (Table I) shows that there is greater negative charge on the "inner" oxygen (O_a) of the peroxyl function; none of the peroxyl radicals has a significant negative charge on the "terminal" oxygen, O_b. On the other hand, the spin density is almost exclusively associated with O_b. Conventional Lewis structures (e.g., **1**) and electronegativity arguments are consistent with these observations: O_a has greater electron density because the adjacent R-group is electron donating; O_b has the unpaired electron, as in structure **1**. Figure 2, together with these data on charge distributions and spin densities, emphasizes that simple pictures based on the relative importance of certain resonance contributors (as in structure **2**) are misleading; i.e., the high polarity observed in structure **1** can be accounted for without invoking structures such as **2**. (Continued use of **2** might be justified by arguing that this structure implies a shift of π-electron density from O_a to O_b, which is true; typically the central oxygen has about 1.9 π-electrons and the terminal oxygen 1.1 π-electrons. However, there is a corresponding shift in the other direction for the σ-electrons, and it is the total electron density which governs the polarity of a species.)

For the 6-31G* optimized geometries, the favored conformations in all cases are those which would be expected from qualitative steric considerations (see the column entitled "relative energies" in Table I). For example, the eclipsed conformation of the methylperoxyl radical, III, is less stable by 5.6 kJ/mol than the staggered conformation, II. This corresponds to the rotational energy barrier around the C–O bond for the methylperoxyl radical and compares well with the 6-31G* rotational barrier for methanol, 5.9 kJ/mol,[35] which in turn is close to the experimentally measured barrier for methanol, 4.6 kJ/mol.[35]

As can be seen in Table II, electron correlation accounts for about one-half of the C–O D_e bond dissociation energy (BDE) in the peroxyls studied. (The BDE is the energy in the reverse process of eq 1.) This is consistent with trends observed in other systems.[36] Thus for the HF/6-311G**//HF/6-31G* calculation for $CH_3\text{-}O\text{-}O^{\bullet} \rightarrow CH_3^{\bullet} + O_2$, the BDE is 60 kJ/mol, whereas at the MP2/6-311G**//HF/6-31G* level it is 110 kJ/mol. Extending the calculations to *third* order in the Møller–Plesset perturbation treatment (MP3/6-311G**//HF/6-31G*) has a relatively small effect by comparison (the BDE increases to 119 kJ/mol). Using a smaller basis set, which is necessary for the larger species, results in an even greater difference between the BDE calculated at the SCF vs the MP2 levels (65 kJ/mol at SCF, 124 kJ/mol at MP2), with again a relatively smaller change when the level is MP3 (130 kJ/mol). In general the differences between the MP2 and MP3 values are of the order of 10 kJ/mol or less, the peroxyl radical being the exception. The basis-set effect is slightly greater, but again the trends are the same.

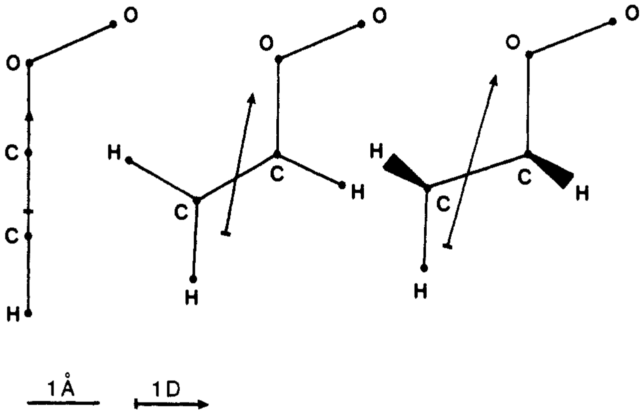

Figure 2. A schematic representation of the magnitude and orientation of the dipole moment vectors of the ethylperoxyl, ethenylperoxyl, and ethynylperoxyl radicals. In each case the length of the vector, denoted by the bold arrow, is proportional to the magnitude of the dipole moment.

The estimated experimental bond energies,[37,38] corrected to D_e,[39] for the C–O bond cleavage of the peroxyl radicals are also given in Table II. The calculated BDE values are consistent with the experimental values in so far as comparisons are possible.

In general, the bond dissociation energies for the homolytic cleavage of the C–O bond are low (89–235 kJ/mol at the MP2/6-31G**//HF/6-31G* level). The highest of these at each level of calculation is that of the ethynylperoxyl radical XVII, H—C≡C—O—O, which, as noted above, also has the shortest C–O bond length of all the species studied. The BDE thus increases as the C–O bond length decreases and as the degree of unsaturation increases; i.e., the greater the degree of unsaturation

---

(35) Reference 30, p 264.

(36) Reference 30, p 273.

(37) Benson, S. W. *J. Am. Chem. Soc.* **1975**, *87*, 972.

(38) Slagle, I. R.; Feng, Q.; Gutman, D. *J. Phys. Chem.* **1984**, *88*, 3648.

(39) Reference 30, p 260.

of the carbon to which the peroxyl group is attached, the larger the BDE. Thus at the MP2/6-311G** level, the BDE is 226 kJ/mol for the ethynylperoxyl radical XVII, 186 kJ/mol for the ethenylperoxyl radical XIV, and 121 kJ/mol for the ethylperoxyl radical V; the corresponding values calculated at the MP2/6-31G** level are 235, 200, and 134 kJ/mol. (While the higher level calculations give smaller BDE, the order of increasing BDE is the same for both levels.)

The BDE is particularly low when the hydrocarbon radical is resonance stabilized. For example, at the MP2/6-31G** level it is 89 kJ/mol for the allylperoxyl (XIX) dissociation,

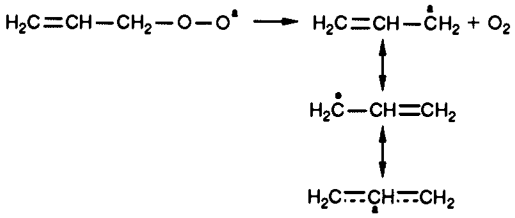

and this is of particular interest for a determination of the energetics and mechanism of the allylperoxyl rearrangement, the study of which is in progress. Similarly, it is 102 kJ/mol for the propynylperoxyl (XXV) dissociation,

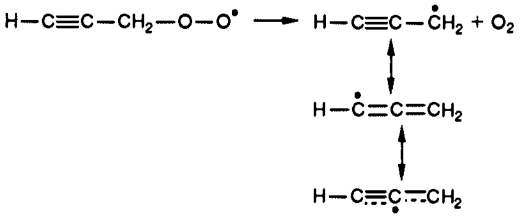

For the corresponding dissociation of the 1-propylperoxyl radical (VIII), it is 136 kJ/mol. In this series the C–O bond lengths do not change (Table I); hence their strengths are essentially constant. However, the stabilities of the unsaturated hydrocarbon radicals are much greater than that for the saturated one.

Among the saturated peroxyl radicals, the methylperoxyl has the lowest BDE (124 kJ/mol at the MP2/6-31G** level), lower than that of the primary radicals, ethylperoxyl (134 kJ/mol) and 1-propylperoxyl (136 kJ/mol); the BDE for the secondary 2-propylperoxyl radical is 146 kJ/mol which is the highest in the series. While secondary hydrocarbon radicals are expected to be more stable than primary ones, due to hyperconjugation, it does not follow that the bond energy would be smaller for the secondary peroxyl radicals unless the assumption is made that primary and secondary peroxyl radicals have the same energy. This is clearly not true, as is indicated by the data of Table I. Thus, the secondary 2-propyl radical XI is more stable (by 11.6 kJ/mol) than the primary 1-propyl radical IX, but the secondary 2-propylperoxyl radical X is also more stable (by 21.5 kJ/mol) than the primary 1-propylperoxyl radical VIII. The bond dissociation energy, then, is greater for the secondary species.

Conclusions

This theoretical study of the structures and properties of peroxyl radicals thus suggests the following conclusions: 1. The effects of electron correlation on the structures of peroxyl radicals are smaller than in the corresponding peroxides. 2. The ⋗C–O bond lengths in the peroxyl radicals are 1.41 to 1.43 Å, while those for =C(—)—O are about 1.38 Å, and for ≡C—O are about 1.32 Å. 3. The O–O bond lengths in peroxyl radicals are about 1.30 Å. 4. The peroxyl radicals are π-radicals. 5. Peroxyl radicals have large dipole moments, generally 2.3–2.6 D. 6. The majority of the negative charge resides on the "inner" oxygen of the peroxyl function, while the spin density is higher on the "terminal" oxygen. 7. Electron correlation accounts for about half of the calculated C–O bond dissociation energy. 8. The C–O bond dissociation energy decreases as the degree of saturation of the carbon to which the peroxyl group is attached increases. 9. The C–O bond dissociation energy decreases when the hydrocarbon radical product is resonance stabilized. 10. The BDE for the methylperoxyl radical is less than that of a primary peroxyl radical, which in turn is less than that of a secondary peroxyl radical.

Acknowledgment. The authors gratefully acknowledge the financial support provided by NSERC to R.J.B. and L.R.C.B. Thanks are also extended to Dr. Ned Porter (Duke University) for helpful discussions. The excellent cooperation of the staff of the Dalhousie University Computing and Information Services throughout this project is acknowledged with gratitude.

Registry No. I, 3170-83-0; II, 2143-58-0; V, 3170-61-4; VIII, 42953-38-8; X, 4399-86-4; XIV, 88181-72-0; XVII, 127646-28-0; XVIII, 4599-48-8; XXV, 127646-29-1.